

Figure S1. The CVs of the electrodeposition.

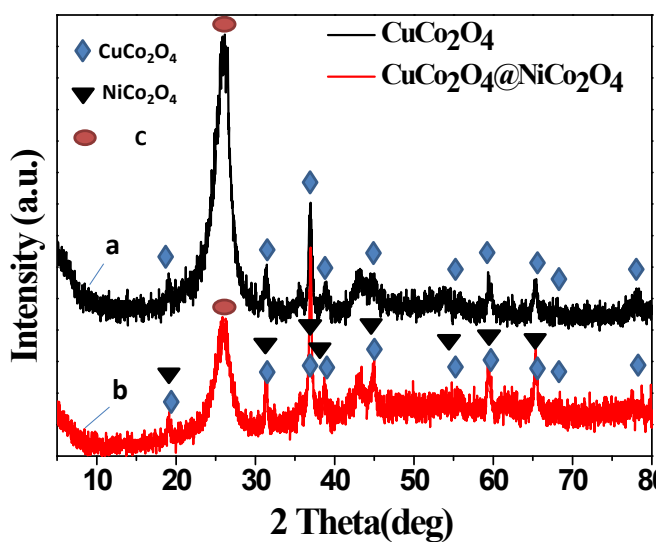


Figure S2. XRD patterns of (a) the bare  $\text{CuCo}_2\text{O}_4$  electrode and (b) the  $\text{CuCo}_2\text{O}_4@/\text{NiCo}_2\text{O}_4$  hybrid electrode.

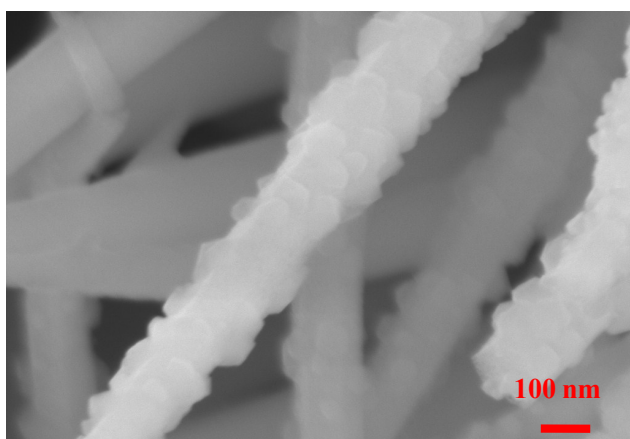


Figure S3. SEM image after the electrodeposition.

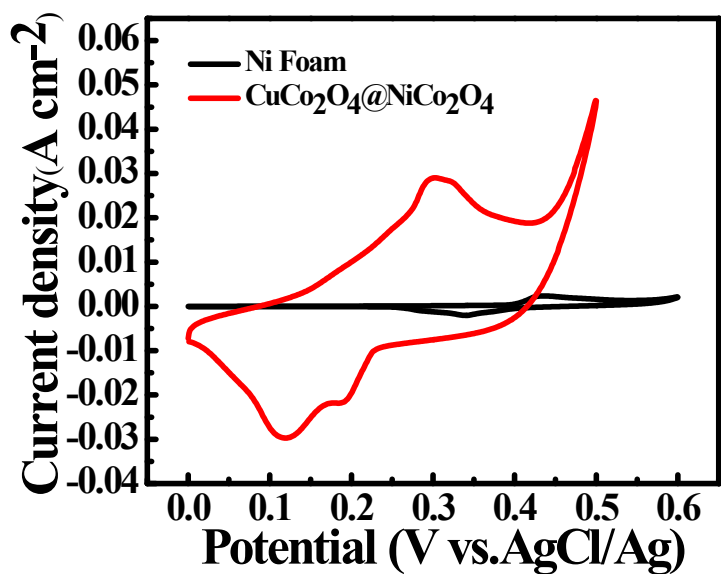


Figure S4. CV curves of the Ni foam and CuCo<sub>2</sub>O<sub>4</sub>@NiCo<sub>2</sub>O<sub>4</sub> hybrid electrodes at a scan rate of 5 mV s<sup>-1</sup>.

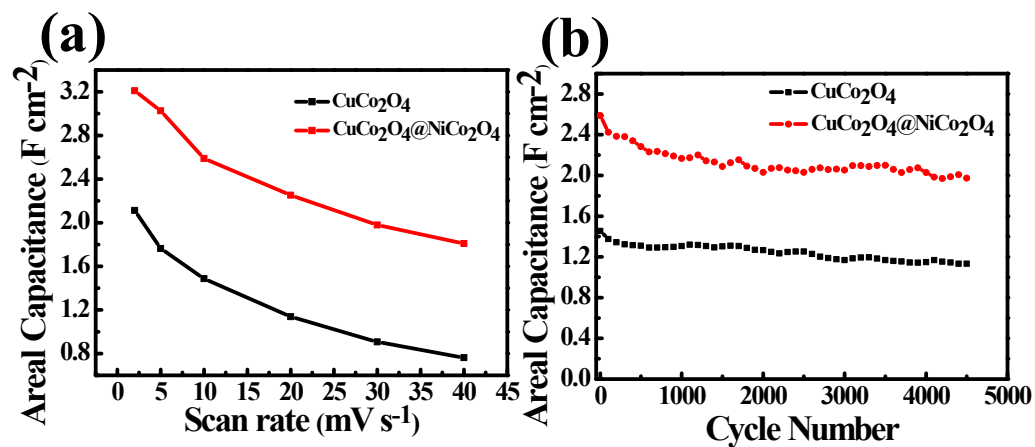


Figure S5. (a) Areal capacitances of CuCo<sub>2</sub>O<sub>4</sub> and CuCo<sub>2</sub>O<sub>4</sub>@NiCo<sub>2</sub>O<sub>4</sub> hybrid electrodes at different current densities. (b) Long-term cycling stability of CuCo<sub>2</sub>O<sub>4</sub> and CuCo<sub>2</sub>O<sub>4</sub>@NiCo<sub>2</sub>O<sub>4</sub> hybrid electrodes at a current density of 10 mA cm<sup>-2</sup>.

